

Fluid Sensing Strategies Adopted in Photonic Devices: A Review

Swagata Samanta^{1,2,*}, Sandeep Kalathimekkad¹, and Shankar Kumar Selvaraja¹

¹ Centre for Nano Science and Engineering, Indian Institute of Science, Bengaluru-560012, Karnataka, India;

² School of Engineering, University of Glasgow, Glasgow-G12 8QQ, Scotland, United Kingdom;
Swagata.Samanta@glasgow.ac.uk (S.S.), sandeepkalat@iisc.ac.in (S.K.), shankarks@iisc.ac.in (S.K.S.)

* Correspondence: Swagata.Samanta@glasgow.ac.uk; Tel.: +44-7514780327

Abstract: Fluid sensing techniques have been proposed by many research groups over the decades. These span a wide range of applications, which include industrial, medical and engineering fields. This review article focuses on the adopted sensing mechanisms in photonic devices for detecting fluids (gas/dissolved gas/liquid/electrolyte). A comparison between different technologies is made taking into account the performance indicators. The advantages and limitations of each of the techniques are highlighted, which will pave the way for future research and development in this area.

Keywords: sensors; fluids; absorption; reflectance; refractometry; photonic device

1. Introduction

Sensors are devices which are capable of detecting changes in physical quantities and can respond to that change. This variable could be temperature, humidity, pressure, light intensity, position, velocity or electric current. Sensors can be broadly classified based on the kind of measurand, material, technology, property, and application [1]. The purpose of this review is to elaborate on the technologies where the physical quantity involved is light intensity. The focus will be on investigating different methodologies adopted by researchers so far for optical sensing. Sensors detecting a change in optical properties offer improved immunity to electromagnetic interference, large bandwidth, and intrinsic safety. Another reason for considering the optical sensors is due to the fact that most of the fluids significant in industrial and environmental applications absorb infrared (IR) or ultraviolet (UV) light. Also, if a choice of substrate material is considered, these sensors are generally transparent in visible, UV, and IR regions of the electromagnetic spectrum. Thus the analysis of samples may be made through absorption, emission or scattering of radiation [2].

Micro ring resonator (MRR), photonic crystal fiber (PCF), photonic crystal waveguide (PCW), photonic crystal ring resonator (PCRR), Mach Zehnder interferometer (MZI), photonic bandgap (PBG) Bragg fiber, long-period fiber grating (LPFG), waveguide Bragg grating (WBG) and porous silicon (PSi) structure are some of the photonic devices which have been used in sensing applications; where, changing the optical properties resulted in variation in spectral characteristics [3–23]. Any change in intensity, frequency, polarization, and phase of reflected or transmitted light as compared to incident light can be used in the sensing mechanism. Photonic structures with large surface area and sensitive to external surrounding has been the primary target of researchers in the field of fluid sensing. Sensing can be realized by monitoring the refractive index changes, intensity, wavelength shift in spectra while varying the concentration of target fluid, temperature of the surrounding environment (using heaters). In order to monitor the fluid concentration and composition, the response and recovery time need to be shorter, as this will reflect the sensor detection efficiency. For a sensor to perform well depends on certain parameters: sensitivity, selectivity, limit of detection, repeatability, response time and recovery time. Low energy consumption, small size and low cost are other factors which determine its effectiveness [24–27]. An ideal fluid sensor should possess high sensitivity, selectivity and stability with a low energy consumption, detection limit, response time and recovery time. In real-world applications, though a sensor need not possess all the ideal characteristics at a time, however, it's obvious these will lead to miniaturized-sensors.

The organization of the article is as follows: Section 2 describes different techniques for sensing fluids, section 3 deals with the advantages and challenges of these adopted techniques, while section 4 draws the concluding remarks and future scope of research.

2. Fluid Sensing Techniques

There are a lot of toxic gases present in the atmosphere, dissolved gases under sea/river, and various liquid and electrolyte mixtures as industry or laboratory wastes, which need to be detected for the sake of the survival of the human race, water life and other living organisms. Water life is affected if the oxygen concentration under water is too low, the same way as human life is suffered if the oxygen concentration is too low in atmosphere. So, there is a need to continuously monitor the concentration of the harmful gases/dissolved gases/electrolytes/vapors as evolved from automotive vehicles and industries. Methane (CH₄), ammonia (NH₃), carbon monoxide (CO), carbon dioxide (CO₂), sulphuric acid (H₂SO₄), hydrogen peroxide (H₂O₂), sodium chloride (NaCl), hydrogen chloride (HCl), different alcohols, and oil, are some fluids to name a few on which people have examined on. Researchers from both industry and academia have proposed different types of fluid sensors, and are still making innovative attempts to improve the performance in terms of sensing parameters. Physical phenomena which have been effectively employed in most of the literature are absorption, reflectance, and refractometry. The basic idea/overview of these physical phenomena are listed in Table 1; while the discussion of detailed study of the sensing techniques based on the physical phenomena, are made in the sub-sections 2.1–2.3.

Table 1. Overview of fluid sensing techniques.

Refractometry	Absorption	Reflectance
measures change in density using wavelength selective device	measures wavelength selective absorption of chemical species	measures reflection spectra
fiber or circuit based configuration	various techniques: FTIR, ATR-FTIR, UV-Vis, XRA, TDLAS, NDIR	relies on density change due to fluid concentration
low/no sensitivity to chemical nature	high sensitivity to chemical nature	low sensitivity to chemical species
high sensitivity to density change	low sensitivity to density change	reasonable sensitivity to density

2.1. Techniques based on refractometry

Refractometry is the technique of measuring the refractive index of substances, especially liquids and gases. Determining the refractive index of sensing fluid finds applications in concentration estimation, contamination assessment, biochemical sensing and physical/chemical process monitoring like online monitoring of fluid concentration [28–32]. The parameters influencing refractive index include concentration, temperature, electric field, magnetic field strength, and pH value. Much research has been done on refractive index sensors with various structures which are influenced by these parameters [5, 6, 10, 33–51]. Introducing a cavity within a photonic crystal waveguide (PCW), and pouring target fluid into it is a common approach of sensing. The working principle involved here is based on evanescent wave sensing utilizing the refractive index change induced by the target fluid. In [33] the authors have used the fluid concentration sensing using PCW approach, where a defect (cavity) is created in the PCW and light (from tunable laser source) is input to pass through it; the output (via collimating lens) is obtained using an optical spectrum analyser. Aqueous H₂SO₄ / H₂O₂ with various concentrations in the cavity change the refractive index; with increased concentration, there is an increment in refractive index, and as a result of which there is a red-shift in wavelength. The average sensitivity in this reported work is 35nm/RIU for H₂SO₄ with a standard deviation of 6.2 and detection limit 0.04. For H₂O₂, the respective values of sensitivity, standard deviation and detection limit are 64.98nm/RIU, 10.87, and 0.02; refractive index of deionized water (DI) water is taken as the reference for both solutions. Although photonic crystal based sensors are compact and provide high resolution of the quantity to detect, they have an inherent limitation of fabrication tolerance. If there is even 1% fabrication error then the structure won't remain periodic; even if the structure guides light there will be huge propagation loss.

Photonic crystal fiber (PCF) is the structure which overcomes the limitation of PCW and possesses unique features like small nonlinearities and low light losses. Due to its waveguide nature and microstructured architecture and the option to fill air core with gases and liquids, it is used as salinity sensor [5, 6]. Figure 1 [5] shows the cross-section of PCF being used as a salinity sensor, where sea water is injected in various concentrations into one of the air holes of the PCF. Refractive index of sea water varies with change in salinity level, which leads to a shift in confinement loss spectrum and resulting in peak wavelength shifts. The variation of refractive index arises when coupling occurs between core and analyte/defect modes in order to meet the phase matching condition. A high sensitivity of 5405 nm/RIU for x-polarization and 5675 nm/RIU for y-polarization is obtained with a detection uncertainty of 0.0037 RIU and high birefringence of the magnitude 10^{-3} .

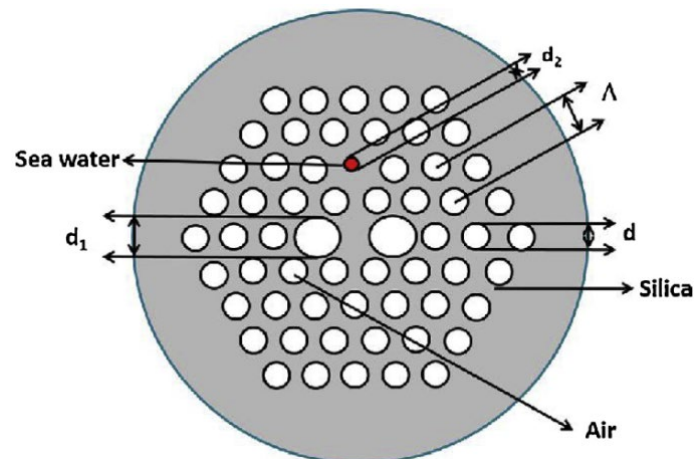


Figure 1. Cross-section of PCF-based sensor [5]

In order to enhance sensitivity and reduce the limit of detection, people have tried modifications on the conventional PCFs. An in-line PCF microfluidic refractometer enabled by a C-shaped PCF (to measure NaCl concentration) [6] yields a sensitivity of 15.08 nm/(1 wt%) and a detection limit of 2.3×10^{-3} wt.% (23 ppm). The cavity/hole arrangement in these PhC-based structures enable to tailor the optical properties and the responsivities; thus, the use of gratings or interferometers help in achieving sensors with higher sensitivity and lower detection limits. Refractive index measurements using hollow-core optical Bragg fiber filled with fluid solutions (with different concentrations) also interests researchers [52]. Liquid-core optical fibers inherently integrate optical detection with microfluidics, thus continuous on-line monitoring of liquid samples in a contained, highly-integrated manner is possible. When the light source is launched into this type of fiber, light frequencies within the Bragg reflector are confined and guided, others irradiates out, thus is a very promising platform for refractive index sensing. Measurement setup of this type of sensor is shown in Figure 2, where two opto-fluidic blocks are used to integrate the liquid core Bragg fiber into the setup. At one end of this fiber, broadband supercontinuum light source is launched through a lens objective; the output is monitored using a grating monochromator.

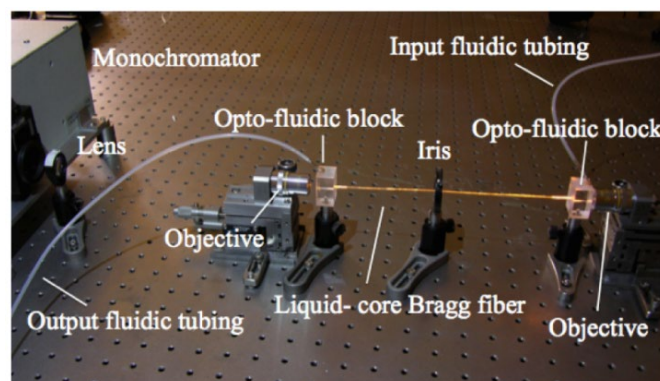


Figure 2. Experimental setup for hollow core Bragg fiber sensor [52]

A sensing element may be formed by adding a periodical transverse pressure on composite optical waveguide forming a pressure-induced long period fiber grating (LPFG). The composite optical waveguide may be composed of a portion of a bare standard single-mode fiber, a teflon-cannula and the medium under test [35]. In this type of sensor setup, the mode field distribution of fundamental core is concentrated in and near fiber core region and it's attenuated in the cladding region. That means, only the cladding is influenced by refractive index of medium under test. There is a variation of the effective index of cladding with a change in the refractive index of medium – this shifts the resonance wavelength in the transmission spectrum. This simple, inexpensive sensor has a sensitivity of 0.128 nm/wt.% in the concentration range from 0% to 25%.

An additional advantage of reduced footprint along with high sensitivity, and a possibility to allow multiplexing is the hallmark for sensors based on ring resonators. Label-free optical sensors and multiplex biosensors [36, 53] are studied by several research groups using a single waveguide ring. But the light source here should have very accurate wavelength with a narrow bandwidth and high stability; practically, this is difficult to achieve. Using a double ring resonator and broadband source [54, 55] will overcome this difficulty. Photonic crystal-based ring resonator (PCRR) takes the advantage both of photonic crystal and ring resonator. Figure 3 [10] is the setup for PCRR-based salinity sensing, where the sensor is placed inside the sea water and emitted optical signal from transmitter is input into it. There is a shift in resonant wavelength with varying sea water concentrations, which finally changes the output signal intensity of the sensor. The receiver collects the output and converts the optical signal into electrical one, which is processed by the signal processing unit and is displayed in the display board. Around 50nm/RIU sensitivity is obtained with this system with a minimum detectable sensitivity of 1% (1g/L).

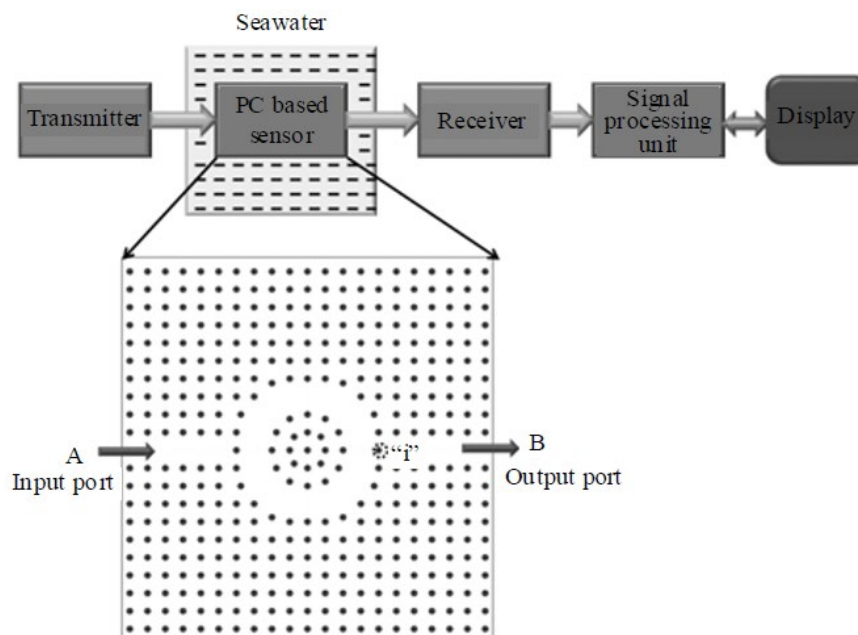


Figure 3. Schematic of PCRR-based salinity sensor [10]

The photonic sensor circuit reported by D. Martens et al. [34] consisted of Mach Zehnder interferometer with one of the arms isolated from the analyte (HCl), while the other is exposed to it. Using an integrated spectral filter with the sensor chip and broadband light source yields a sensitivity of 2100 nm/RIU and a detection limit of 6×10^{-6} RIU. A ring-coupled Mach-Zehnder interferometer (MZI) allows achieving high sensitivity with a large measurement range [56, 57], but the small detection power limits these structures. A modified hybrid structure consisting of reflective MZI and ring resonator will resolve this issue with the cost of being a bit expensive [9]. The reflective MZI, when cascaded with the through port of a MRR produces a Vernier effect with a high output power. The schematic of the setup to measure spectral response of this sensor is shown in Figure 4. A tunable laser source is used here as the light source, which is coupled into the input port (port 1) of the fiber coupler through a polarizer, and splits into two arms of the reflective MZI. The reflective light from port 2 interferes with the one from port 3 at port 4. Finally, the light is coupled into the sensing ring

through a grating coupler (port 5). The output signal from the through port (port 6) is finally received by the power sensor (Agilent 81634A). Table 2 lists some of the notable works based on refractive-index sensing.

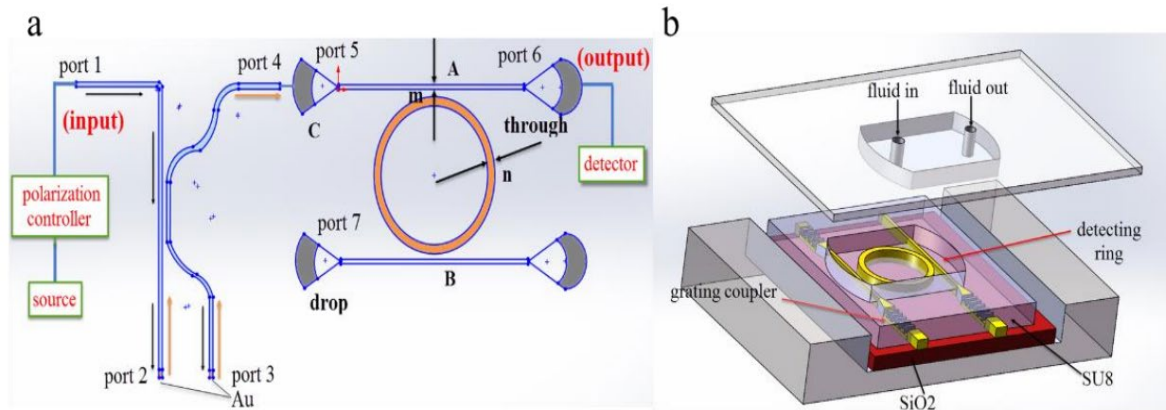


Figure 4. Schematic of the cascaded reflective MZI and MRR (a) whole structure; (b) microring resonator [9]

Table 2. Work related to refractive index-based detection techniques.

Instrument/ tool used	Device	Fluid	Wavelength (nm)	Sensitivity	Detection limit	Standard deviation
refractometer (ATAGO, Japan) [27]	PCW	H ₂ SO ₄	1550	35nm/RIU	0.04 RIU	6.2
		H ₂ O ₂		64.98nm/RIU	0.02 RIU	10.87
- [5]	PCF	Sea water	NIR (broadband source)	5405 (x-pol.), 5675 (y-pol.)	0.0037 RIU	-
refractometer (enabled by C- shaped fiber) [6]	PCF	NaCl	NIR (broadband source)	15.08 nm (1 wt. %)	2.3× 10 ⁻³ wt% (23ppm)	0.9991
spectrometer [52]	PBG Bragg fibers	NaCl	589	2.6 nm/wt. %	-	-
OSA [35]	LPFG	NaCl	500 to 1700 (supercontinuum source)	0.128 nm/wt.%	-	0.9905
power meter [30]	MRR	NaCl	NIR (tunable laser source)	49.75 nm/RIU	-	0.72
signal processing	PCRR	Sea	NIR	1 g/L	-	-

unit, display board [10]		water				
integrated biosensing platform [34]	MZI	HCl	NIR (broadband source)	2100 nm/RIU	6×10^{-6} RIU	0.02
power sensor (Agilent 81634A) [9]	MZI and MRR	NaCl	1585 (broadband source)	1892 dB/RIU	5.28×10^{-6} RIU	-
tunable laser (Keysight 81960A), photodetector (Keysight 81636B) [48]	Slot ring resonator	KCl, glycerin, KHCO_3	1550	476 nm/RIU (maximum)	1.05×10^{-5} RIU	-
Tunable laser, photodetector, power meter [51]	Slotted MRR	Acetel- yne	NIR	490 nm/RIU	-	-

2.2. Techniques based on absorption

Optical fluid sensing techniques based on absorption measure the amount of light that is absorbed by a sample at a particular wavelength, and follows Beer-Lambert law. Researchers have adopted various approaches which include non-dispersive infrared (NDIR) absorption technique, Fourier transform infrared (FTIR), attenuated reflection Fourier transform infrared (ATR-FTIR), ultraviolet-visible (UV-Vis), X-ray absorption (XRA), quantum cascaded laser (QCL) and tunable diode laser absorption spectroscopies (TDLAS). Dispersive infrared absorption spectra cover a wide range of wavelengths extending from 2–20 μm ; the positions and heights of wavelength in the absorption spectra help in determining the gases and their concentrations respectively. The available instruments based on this technique have the downside of being bulky, expensive, and fragile, thus limiting the use within laboratories only. The IR detector, along with fixed narrow-band optical filter used in NDIR spectroscopy on the other hand, enable to detect gases in a narrow wavelength range, thus are smaller, less expensive, and robust. This technique finds its utility where the absorption lines between various gases overlap, and still there is need to measure the concentration of target gas. Another advantage of NDIR spectroscopy is its low energy consumption; disadvantage of this technique is spectral interference and high detection limit. With this method, D. Pergande et al. [58] in 2011 presented an optical gas sensor using two-dimensional macroporous silicon photonic crystal (PhC) gas cells. In order to measure the gas absorption, PhC membranes are placed in between two BaF_2 light guiding rods; the gas analyte (CO_2) flow being perpendicular to the light path through the PhC membrane. As can be seen from the setup (Figure 5), only thermal radiation source and a pyrodetector with an IR bandpass filter is required for the absorption measurement. The broadband thermal emitter is filtered by the IR bandpass filter. There is an edge filter (consisting of sapphire window) placed in front of the pyroelectric detector; a lock-in amplifier enables measuring the signal of this detector. It is noticed that there is an enhancement of CO_2 infrared absorption in PhC gas cell by a factor of 2.6 to 3.5 compared to an empty cell. This enhancement is due to slow light inside the photonic crystal gas cell.

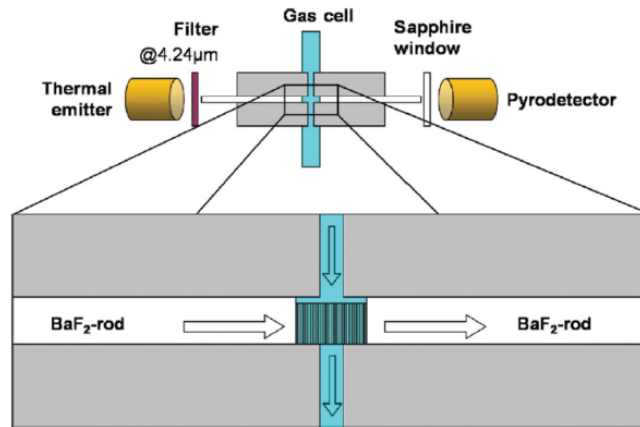


Figure 5. Optical setup for gas absorption measurements [58]

Ammonia gas, which can be smelled when its level exceeds 0.04–57 ppmv, starts affecting human health once the level reaches to 50–100ppmv [59, 60]; so sensors with an ability to detect low concentration ammonia gas become important. Another critical application of the ammonia sensor is in the semiconductor fabrication. The yield of optoelectronic products in semiconductor industries also depends on the concentration of ammonia gas. Researchers have developed a mesoporous silica material (Al-MCM-41(50)/BG) to measure low-level ammonia gas (detection limit of 0.185 ppmv) [61] using an UV-Vis diffuse reflection accessory spectroscopic instrument. X-ray absorption spectroscopy is another approach of detecting fluids. This technique investigates local structures of liquid samples with element analysis; however, the thickness of thin liquid layers need to be optimized for appropriate absorbance around 0.3–0.7 and keep the sample thickness flat within a photon beam. Reliable transmission-mode XAS spectra of liquid samples is obtained by measuring position-dependent O K-edge transmission-mode XAS spectra of liquid water [62]. S. Content et al. [63] detected nitroaromatic molecules (nitrobenzene, 2,4-dinitrotoluene, 2,4,6-tri-nitrotoluene) in air by photoluminescence quenching of nanocrystalline porous silicon; the absorption spectra is analysed using Fourier transform infrared (FTIR) spectroscopy. They reported a detection limit of 500, 2 and 1 ppb for nitrobenzene, 2,4-dinitrotoluene (DNT), and 2,4,6-tri-nitrotoluene (TNT) respectively.

Although FTIR is capable of identifying functional groups, monitoring all types of samples (solids, liquids, gases) continuously with high precision and quantifying large concentration spans, the samples require complex preparation. To overcome this drawback, ATR (attenuated reflection) mode is used, where the samples are placed undiluted on the ATR crystal, thus simpler and faster. This mode also overcomes the drawback of strong water absorption in the IR region, which would make the other weaker spectral bands of interest unclear [64]. However, in order to obtain high quality spectra, there should be a good contact between the sample and the ATR crystal, and the refractive index of the crystal should be greater than that of the sample. Detection technology based on attenuated reflection Fourier transform infrared (ATR-FTIR) spectroscopy has been implemented by K. L. A. Chan et al. [2] for direct imaging and mixing of H₂O and D₂O. The chemical imaging of the liquid mixture flowing in microfluidic device is done using an IR focal plane array (FPA) detector, the ATR crystal surface being the base of the device (Figure 6).

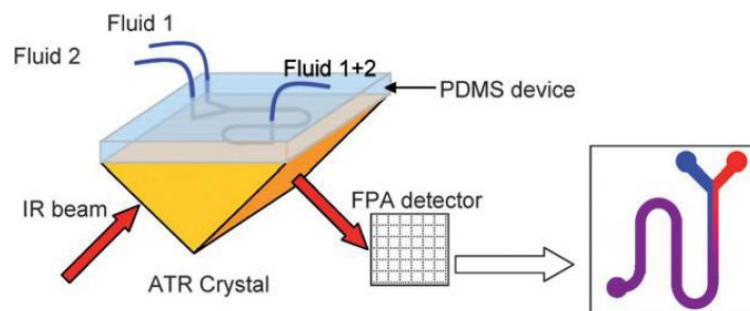


Figure 6. Schematic of ATR-FTIR imaging system and integration with a planar, chip-based microfluidic device [2]

One of the inherent limitations of FTIR techniques is low spectral and time resolution; to develop highly selective and fast response a technique called TDLAS comes into play. Wavelength-modulated absorption of diode laser light has the advantage of low detection limit and low power requirement. This method has been used to monitor HCl concentration in a plasma reactor for etching polysilicon in Cl₂/HBr plasmas [65]. However, this diode based spectroscopy cannot be operated at cryogenic temperatures. There are also issues with long-term reliability with spectral characteristics, mode purity, and multi-mode behavior in some cases [66]. Other constraints like limited power output from light source (as present in FTIR or TDLAS) are overcome by employing Quantum cascade laser absorption spectroscopy. This technique also has the advantages of operating at cryogenic temperatures, has high spectral purity and relatively high power output. Notable works can be found in literature using this technique [66–68]. Researchers [69] have used this technique for measuring the concentration of atmospheric N₂O, CO, CO₂ isotopes; however, the high price of the QCL lasers limits the use of these techniques to niche applications. Some of the noted works involving absorption-based methods are listed in Table 3.

Table 3. Work related to absorption-based detection techniques.

Technique	Device	Fluid	Wave-length	Sensitivity	Detection limit
NDIR [58]	PhC gas cells	CO ₂	4.24 μm	Enhancement of CO ₂ IR absorption by a factor of 2.6 to 3.5 as compared to empty cell	-
ATR-FTIR [2]	inverted ATR crystal with PDMS-based microfluidic mixing device	H ₂ O, D ₂ O, HDO	-	-	-
XAS [62]	-	liquid H ₂ O	-	-	-
FTIR [63]	Porous silicon chip	Nitrobenzene, DNT, TNT	-	-	500ppb (nitrobenzene), 2ppb (DNT), 1ppb (TNT)
TDLAS [65]	-	HCl	1.79 μm	-	4×10 ⁻⁶ RIU
UV-Vis DRA [61]	mesoporous silica	NH ₃	0.63 μm	0.0262	0.185 ppmv
QCLAS [66]	-	CO ₂	4.3 μm	-	-

2.3. Techniques based on reflectance

Reflectance-based spectroscopy is the technique of measuring light reflected from the sample; that is, the optical properties of the sample are extracted from reflected light. So, there is an influence of angle of incidence and orientation for reflected wavelengths to change. Structures like photonic crystals, porous silicon, and Bragg reflector structured porous silicon have been used as sensor elements in various sensing applications like chemical vapor sensing, ionic strength sensing, and interference color change sensing. For ionic sensing, sophisticated indicator probes and instrumental readout are required. Also, there should not be any interference by pH values or dissolved CO₂ and O₂. A polyacrylamide hydrogel based photonic crystal sensor as reported by C. Fenzl et al. [70] has these merits, and is capable of sensing ionic strength by giving distinct color images. The hydrogel immersed in varying concentrations of salt solutions of NaCl, HCl, H₂SO₄ were used to study the effect of ionic strength on wavelength of reflected light of colloidal photonic crystals. The setup for recording the reflection spectra used here consists of a xenon lamp (acts as the source of illumination) and a fiber waveguide (placed perpendicular to this lamp) connected to a spectrometer (Ocean Optics, Dunedin, FL).

Due to the influence of porous silicon on reflectance and large surface area, they are being used in sensing different gases/vapors [71–73]. However, people have mentioned about their inability to detect an extremely localized variation in the reflectance in a sample. Distributed Bragg grating structured porous silicon (DBG PSi), which exhibits a high reflectivity stop band due to interference in the optical reflectance spectrum, will solve this problem. Here, a specific interference color corresponds to wavelengths of the stop band. By using this color difference image technique for DBR PSi, ethanol vapor is detected [12]. The DBR PSi is exposed to various concentrations; with increase in vapor concentration lightness in color-difference images increases, which means that the degree of interference color change depends on the vapor concentration. Minimum and maximum color response obtained were 90% at 65ppm and 750% at 22,500ppm respectively. A high sensitivity, faster recovery and response time were also obtained using this image technique.

Reflectivity measurement which will result in high repeatability and sensitivity along with easy positioning and flexibility always draw attention to the researchers [11, 74]. An experimental setup where sensor can be located where ever desired is shown by Karacali et al. [11]. A tungsten halogen lamp acts as the light source; bifurcated optical multimode fiber (BFMF) is used to feed this light source to the sensor and extract the reflected signal from the sensor. Splice bushing (SB) connects the sensor and BFMF. Two erlenmeyer flasks are used: the sensor coupled with MMF patch cord is placed inside one of them and is used as a test cell, while another one is filled with organic solvents and is used to produce solvent vapor. The vacuum pump maintains a stable ambient atmosphere of the solvent vapor in the test cell and removes solvent vapor out of the test cell by means of solely nitrogen gas flow. For the reflectivity spectrum measurement, first of all a reference signal is detected under carrier gas flow (nitrogen); next reflected signal from gas sample is measured via the constant nitrogen gas flow. The final result is normalizing the reflected signal from sample with reference signal. Reflectivity measurements of alcohol (methanol, ethanol, 2-butanol) using this porous silicon based sensor resulted in higher repeatability than the conventional one, though the sensitivity remained same in both the cases. Table 4 details the reported detection techniques based on reflectance.

Table 4. Work related to reflectance-based detection techniques.

Technique/ Instrument used	Device	Fluid	Wave- length	Sensitivity	
reflection spectroscopy (SpectraSuite) [70]	polyacrylamide hydrogel-based PhC sensor	NaCl, HCl, H ₂ SO ₄	-	Min detectable sensitivity is 0.03 logarithmic units	Ionic strength sensing
color-difference image technique [12]	distributed Bragg reflector structured porous silicon	Ethanol vapor	-	maximum color response was 750% at 22,500ppm; minimum response was 90% at 65ppm	Interference color change sensing

spectrometer (Ocean Optics NIR512) [11]	Porous Si sensor	Alcohol (methanol, ethanol, 2- butanol	900 to 1500 nm	-	Chemical gas vapor sensing
--	------------------	---	-------------------	---	-------------------------------

3. Advantages and limitations of the adopted Techniques

This section summarizes the performance of all the aforementioned adopted techniques used in sensing photonic devices. The advantages and challenges involved with these techniques are put in a nutshell in the Table below:

Table 5. Advantages and limitations of adopted sensing techniques.

Techniques	Advantages	Limitations
PhC-based	<ul style="list-style-type: none"> • Highly sensitive • Low detection limits 	<ul style="list-style-type: none"> • High manufacturing costs • Complex procedure
hollow core optical fibre-based	<ul style="list-style-type: none"> • Enables integration • Enables continuous monitoring • Cost-effective 	<ul style="list-style-type: none"> • Cross-sensitivity
ring-resonator-based	<ul style="list-style-type: none"> • Reduced footprint • Highly sensitive • Enables multiplexing 	<ul style="list-style-type: none"> • Stability hard to achieve • Bandwidth limited
PCRR-based	<ul style="list-style-type: none"> • High sensitivity and high stability • Best of both worlds 	<ul style="list-style-type: none"> • Expensive
ring-coupled MZI-based	<ul style="list-style-type: none"> • Highly sensitive • Wide measurement range 	<ul style="list-style-type: none"> • Small detection power
dispersive IR absorption-based	<ul style="list-style-type: none"> • Highly sensitive 	<ul style="list-style-type: none"> • Bulky • Expensive • Fragile
NDIR-based	<ul style="list-style-type: none"> • Small and robust • Less-expensive • Low energy consumption 	<ul style="list-style-type: none"> • Spectral interference • Higher detection limits
FTIR-based	<ul style="list-style-type: none"> • Highly specific 	<ul style="list-style-type: none"> • Requires complex sample preparation
ATR-FTIR-based	<ul style="list-style-type: none"> • Simpler and faster 	<ul style="list-style-type: none"> • Low spectral and time resolution
diode-based spectroscopy	<ul style="list-style-type: none"> • Low detection limits • Low power requirements 	<ul style="list-style-type: none"> • Cannot be operated at cryogenic temperatures • Issues with long-term reliability of spectral characteristics and mode purity
QCLAS-based	<ul style="list-style-type: none"> • Cryogenic operation possible 	<ul style="list-style-type: none"> • Expensive

	<ul style="list-style-type: none"> • High spectral purity • Relatively high power output 	
DBR Psi-based	<ul style="list-style-type: none"> • Highly sensitive • Faster recovery and response time 	<ul style="list-style-type: none"> • Thermal instability

4. Conclusions and Future Scope of Research

In this review paper, we have discussed the varied methodologies adopted in scientific and industrial protocols for gas/fluid sensing based on optical methods. Detecting and analysing various atmospheric gases, electrolytes, liquids, and dissolved gases in liquids are essential for each separate and specific application. This can be as wide as medicine, food technology, environmental monitoring for pollutants, industrial safety and defence. Preservation of quality for aquatic life or detection of danger to human health, any of such distinctive application would each require some unique parameter in sensing. The classification we have adopted is based on technologies employed in the design of the sensor; there are still wide ranges of possibilities in realisation of high sensitivity, considerable specificity, but at the same time not compromising on the values of limit of detection. The choice of the sensing platform must be application-specific and since continuous monitoring of the chemical is vital when it comes to analysing reaction chemistry, an obvious path to take is incorporating more than one method to form a multi-nodal and multi-analyte sensing system. Owing to the advantages of optical methods, researchers have adopted several techniques based on the optical properties. Hence an exhaustive study of these techniques along with their exclusive and extensive advantages and challenges is discussed here. Taking into account the drawbacks of the optical methods, the researchers should focus on resolving the high cost and difficulty in device miniaturization. Challenges in detecting real-time fluids like locating very low levels of fluids and difficulty in tracking their movement are still prevalent and this is something that they should take care of. Also in the larger Internet-of-Things (IoT), integration of two or more techniques must be the way to go for utilising complementary properties of each other in order to improve the device performance. Playing with novel device structures will also do the same; for example, a Mach-Zehnder-enhanced off-axis micro ring resonator will significantly improve the performance in terms of sensitivity and limit of detection.

Acknowledgment

The authors would like to acknowledge Shell for providing financial support to conduct the research.

Author Contributions

S.S. did the literature survey and wrote the review article; S.K.S. supervised in preparing the manuscript; S. K. checked the technical correctness of the paper.

References

1. Ahuja, D.; Parande, D. Optical sensors and their applications. *Journal of Scientific Research and Reviews* **2012**, *1*, 060–068.
2. Chan, K.L.A.; Gulati, S.; Edel, J.B.; Mello, A.J.; Kazarian, S.G. Chemical imaging of microfluidic flows using ATR-FTIR spectroscopy. *Lab on a Chip* **2009**, *9*, 2909–1913. DOI: 10.1039/b909573j
3. Yalcin, A.; Popat, K.C.; Aldridge, J.C.; Desai, T.A.; Hryniewicz, J.; Chbouki, N.; Little, B.E.; King, O.; Chu, V.V.S.; Gill, D.; Washburn, M.A.; Goldberg, B.B. Optical sensing of biomolecules using microring resonators. *IEEE Journal of Selected Topics in Quantum Electronics* **2006**, *12*, 148–155. DOI: [10.1109/JSTQE.2005.863003](https://doi.org/10.1109/JSTQE.2005.863003)

4. White, I.M.; Fan, X. On the performance quantification of resonant refractive index sensors. *Optics Express* **2008**, *16*, 1020–1028. DOI: 10.1364/OE.16.001020
5. Vigneswaran, D.; Ayyanar, N.; Sharma, M.; Sumathi, M.; Mani Rajan, M.S.; Porsezian, K. Salinity Sensor Using Photonic Crystal Fiber. *Sensors and Actuators A* **2018**, *269*, 22–28. DOI: 10.1016/j.sna.2017.10.052
6. Wu, C.; Tse, M.L.V.; Liu, Z.; Guan, B.O.; Zhang, A.P.; Lu, C.; Tam, H.Y. In-line microfluidic integration of photonic crystal fibres as a highly sensitive refractometer. *Analyst* **2014**, *139*, 5422–5429. DOI: 10.1039/c4an01361a
7. Gabalis, M.; Urbonas, D.; Petruskevicius, R. A perforated microring resonator for optical sensing applications. *Journal of Optics* **2014**, *16*, 105003. DOI: 10.1088/2040-8978/16/10/105003
8. Cunningham, B.T.; Zhang, M.; Zhuo, Y.; Kwon, L.; Race, C. Recent Advances in Biosensing With Photonic Crystal Surfaces: A Review. *IEEE Sensors* **2016**, *16*, 3349–3366. DOI: 10.1109/JSEN.2015.2429738
9. Zhu, H.H.; Yue, Y.H.; Wang, Y.J.; Zhang, M.; Shao, L.Y.; He, J.J.; Li, M.Y. High-sensitivity optical sensors based on cascaded reflective MZIs and microring resonators. *Optics Express* **2017**, *25*, 28612. DOI: 10.1364/OE.25.028612
10. Robinson, S.; Nakkeeran, R. PC Based Optical Salinity Sensor for Different Temperatures. *Photonic Sensors* **2012**, *2*, 187–192. DOI: 10.1007/s13320-012-0055-6
11. Karacali, T.; Hasar, U.C.; Ozbek, I.Y.; Oral, E.A.; Efeoglu, H. Novel Design of Porous Silicon Based Sensor for Reliable and Feasible Chemical Gas Vapor Detection. *Journal of Lightwave Technology* **2013**, *31*, 295–305. DOI: 10.1109/JLT.2012.2230246
12. Park, S.H.; Seo, D.; Kim, Y.Y.; Lee, K.W. Organic vapor detection using a color-difference image technique for distributed Bragg reflector structured porous silicon. *Sensors and Actuators B* **2010**, *147*, 775–779. DOI: 10.1016/j.snb.2010.03.075
13. Klimov, N.N.; Mittal, S.; Berger, M.; Ahmed, Z. On-chip silicon waveguide Bragg grating photonic temperature sensor. *Optics Letters* **2015**, *40*, 3934–3936. DOI: 10.1364/OL.40.003934
14. Yu, W.; Lang, T.; Bian, J.; Kong, W. Label-free fiber optic biosensor based on thin-core modal interferometer. *Sensors and Actuators B: Chemical* **2016**, *228*, 322–329. DOI: 10.1016/j.snb.2016.01.029
15. Nitkowski, A.; Chen, L.; Lipson, M. Cavity-enhanced on-chip absorption spectroscopy using microring resonators. *Optics Express* **2008**, *16*, 11930–11936. DOI: 10.1364/OE.16.011930
16. Sumetsky, M.; Windeler, R.S.; Dulashko, Y.; Fan, X. Optical liquid ring resonator sensor. *Optics Express* **2007**, *15*, 14376–14381. DOI: 10.1364/OE.15.014376
17. Ranacher, C.; Tortschanoff, A.; Consani, C.; Moridi, M.; Grille, T.; Jakoby, B. Photonic Gas Sensor Using a Silicon Strip Waveguide. *Proceedings* **2017**, *1*, 547; DOI: 10.3390/proceedings1040547
18. Leon, M. J. B. M.; Kabir, M.A. . Design of a liquid sensing photonic crystal fiber with high sensitivity, birefringence & low confinement loss. *Sensing and Bio-Sensing Research* **2020**, *28*, 100335. DOI: 10.1016/j.sbsr.2020.100335
19. Islam, M.S.; Paul, B.K.; Ahmed, K.; Asaduzzaman, S.; Islam, M.I.; Chowdhury, S.; Sen, S.; Bahar, A.N. Liquid-infiltrated photonic crystal fiber for sensing purpose: Design and analysis. *Alexandria Engineering Journal* **2018**, *57*, 1459–1466. DOI: 10.1016/j.aej.2017.03.015
20. Lai, W.C.; Chakravarty, S.; Zou, Y.; Chen, R.T. Multiplexed detection of xylene and trichloroethylene in water by photonic crystal absorption spectroscopy. *Optics Letters* **2013**, *38*, 3799–3802. DOI: 10.1364/ol.38.003799
21. Santi, S.; Musi, V.; Descrovi, E.; Paeder, V.; Francesco, J. D.; Hvozdar, L.; Wal, P. V. D.; Lashuel, H. A.; Pastore, A.; Neier, R.; Herzig, H. P. Real-time Amyloid Aggregation Monitoring with a Photonic Crystal-based Approach. *ChemPhysChem* **2013**, *14*, 3476–3482. DOI: 10.1002/cphc.201300633
22. Rodriguez, G. A.; Aurelio, D.; Liscidini, M.; Weiss, S. M. Bloch surface wave ring resonator based on porous silicon. *Applied Physics Letters* **2019**, *115*, 011101. DOI:10.1063/1.5093435
23. Ryckman, J. D.; Liscidini, M.; Sipe, J. E.; Weiss, S. M. Porous silicon structures for low-cost diffraction-based biosensing. *Applied Physics Letters* **2010**, *96*, 171103. DOI:10.1063/1.3421545
24. Yunusa, Z.; Hamidon, M.N.; Kaiser, A.; Awang, Z. Gas Sensors: A Review. *Sensors and Transducers* **2014**, *168*, 61–75.

25. Pan, J.; Cha, T.G.; Chen, H.; Choi, J.H. Carbon nanotube-based optical platforms for biomolecular detection. In *Carbon Nanotubes and Graphene for Photonic Applications*, Yamashita, S.; Saito, Y.; Choi, J.H., Eds.; Woodhead Publishing Limited, 2013; pp. 270–297. DOI: 10.1533/9780857098627.3.270
26. Liu, X.; Cheng, S.; Liu, H.; Hu, S.; Zhang, D.; Ning, H. A Survey on Gas Sensing Technology. *Sensors* **2012**, *12*, 9635–9665. DOI: 10.3390/s120709635
27. Talataisong, W.; Ismaeel, R.; Brambilla, G. Review of Microfiber-Based Temperature Sensors. *Sensors* **2018**, *18*, 461. DOI: 10.3390/s18020461
28. Beuthan, J.; Minet, O.; Helfmann, J.; Herrig, M.; Müller, G. The spatial variation of the refractive index in biological cells. *Physics in Medicine and Biology* **1996**, *41*, 369–382. DOI: 10.1088/0031-9155/41/3/002
29. Singh, S. Refractive index measurement and its applications. *Physica Scripta* **2002**, *65*, 167–180. DOI: 10.1238/Physica.Regular.065a00167
30. Fan, X.; White, I.M.; Shopova, S.I.; Zhu, H.; Suter, J.D.; Sun, Y. Sensitive optical biosensors for unlabeled targets: A review. *Analytica Chimica Acta* **2008**, *620*, 8–26. DOI: 10.1016/j.aca.2008.05.022
31. Dahlin, A.B. *Plasmonic Biosensors- An Integrated View of Refractometric Detection*, IOS Press, 2012; pp. 1–293. DOI: 10.3233/978-1-60750-966-0-i
32. Yu, H.; Xiong, L.; Chen, Z.; Li, Q.; Yi, X.; Ding, Y.; Wang, F.; Lv, H.; Ding, Y. Solution concentration and refractive index sensing based on polymer microfiber knot resonator. *Applied Physics Express* **2014**, *7*, 022501. DOI: 10.7567/APEX.7.022501
33. Painam, B.; Kaler, R.S.; Kumar, M. Photonic Crystal Waveguide Biochemical Sensor for the Approximation of Chemical Components Concentrations. *Plasmonics* **2016**, *12*, 899–904. DOI: 10.1007/s11468-016-0341-z
34. Martens, D.; Priego, P.R.; Murib, M.S.; Elamin, A.A.; Guerrero, A.B.G.; Stehr, M.; Jonas, F.; Anton, B.; Hlawatsch, N.; Soetaert, P.; Vos, R.; Stassen, A.; Severi, S.; Roy, W.V.; Bockstaele, R.; Becker, H.; Singh, M.; Lechuga, L.M.; Bienstman, P. A low-cost integrated biosensing platform based on SiN nanophotonics for biomarker detection in urine. *Analytical Methods* **2018**, *10*, 3066. DOI: 10.1039/c8ay00666k
35. Shi, S.; Zhou, X.; Zhang, Z.; Yin, C.; Liu, Y. An optical solution concentration sensor based on periodical pressure-induced long-period fiber gratings. Symp. on Photonics and Optoelectronics, Shanghai, China, 21–23 May 2012. DOI: 10.1109/SOPO.2012.6270941
36. Wang, L.; Kodeck, V.; Vlierberghe, S.V.; Ren, J.; Teng, J.; Han, X.; Jian, X.; Baets, R.; Morthier, G.; Zhao, M. A Low Cost Photonic Biosensor Built on a Polymer Platform. Proceeding of SPIE-OSA-IEEE Asia Communications and Photonics, Shanghai, China, 13–16 Nov 2011. DOI: 10.1117/1.12.904188
37. Luan, N.; Ding, C.; Yao, J. A Refractive Index and Temperature Sensor Based on Surface Plasmon Resonance in an Exposed-Core Microstructured Optical Fiber. *IEEE Photonics* **2016**, *8*, 4801608. DOI: 10.1109/JPHOT.2016.2550800
38. Prasad, P.R.; Selvaraja, S.K.; Varma, V. Real-time compensation of errors in refractive index shift measurements of microring sensors using thermo-optic coefficients. *Optics Express* **2018**, *26*, 13461–13473. DOI: 10.1364/OE.26.013461
39. Zhang, J.; Pu, S.; Rao, J.; Yao, T. Refractive index and temperature sensors based on no-core fiber cascaded with long period fiber grating. *Journal of Modern Optics* **2018**, *65*, 1098–1103. DOI: 10.1080/09500340.2018.1424360
40. Yin, B.; Wu, S.; Wang, M.; Liu, W.; Li, H.; Wu, B.; Wang, Q. High-sensitivity refractive index and temperature sensor based on cascaded dual-wavelength fiber laser and SNHNS interferometer. *Optics Express* **2019**, *27*, 252–264. DOI: 10.1364/OE.27.000252
41. Song, J.; Luo, X.; Kee, J.S.; Han, K.; Li, C.; Park, M.K.; Tu, X.; Zhang, H.; Fang, Q.; Jia, L.; Yoon, Y.J.; Liow, T.Y.; Yu, M.; Lo, G.Q. Silicon-based optoelectronic integrated circuit for label-free bio/chemical sensor. *Optics Express* **2013**, *21*, 17931–17940. DOI: 10.1364/OE.21.017931
42. Zhu, J.H.; Huang, X.G.; Xu, W.; Chen, L.X. Plasmonic optical switches based on Mach-Zender interferometer. *Physics of Plasmas* **2011**, *18*, 72112–72116. DOI: 10.1063/1.3614521
43. Rao, J.; Pu, S.; Yao, T.; Su, D. Ultrasensitive Magnetic Field Sensing Based on Refractive-Index-Matched Coupling. *Sensors* **2017**, *17*, 1590. DOI: 10.3390/s17071590
44. Togo, H.; Mochizuki, S.; Kukutsu, N. Optical Fiber Electric Field Sensor for Antenna Measurement. *NTT Technical Review* **2009**, *7*, 1–6.

45. Hong, C.Y.; Chieh, J.J.; Yang, S.Y.; Yang, H.C.; Horng, H.E. Simultaneous identification of the low-field-induced tiny variation of complex refractive index for anisotropic and opaque magnetic-fluid thin film by a stable heterodyne Mach–Zehnder interferometer. *Applied Optics* **2009**, *48*, 5604–5611. DOI: 10.1364/AO.48.005604
46. Kniazkov, A.V.; Davydov, S.N. An electric field sensor based on reflected light intensity modulation from electro-optical media. *Optical Memory and Neural Networks* **2017**, *26*, 145–149. DOI: 10.3103/S1060992X17020096
47. Gu, B.; Yin, M.J.; Zhang, A.P.; Qian, J.W.; He, S. Low-cost high-performance fiber-optic pH sensor based on thin-core fiber modal interferometer. *Optics Express* **2009**, *17*, 22296–22302. DOI: 10.1364/OE.17.022296
48. Mere, V.; Muthuganesan, H.; Kar, Y.; Kruijsdijk, C.V.; Selvaraja, S. K. On-chip Chemical Sensing using Slot-waveguide based Ring Resonator. *IEEE Sensors Journal* **2020**, *20*, 5970–5975. DOI: 10.1109/JSEN.2020.2974502
49. Jágerská, J.; Zhang, H.; Diao, Z.; Thomas, N. L.; Houdré, R. (2010). Refractive index sensing with an air-slot photonic crystal nanocavity. *Optics Letters* **2010**, *35*, 2523–2525. DOI:10.1364/ol.35.002523
50. Mere, V.; Muthuganesan, H.; Dasgupta, P.; Bhat, N.; Selvaraja, S. K. Silicon Slot Waveguide based Bulk Refractive Index Sensing of Electrolyte and Carbohydrate. European Conference on Integrated Optics (ECIO), Ghent, Belgium, 2019.
51. Robinson, J. T.; Chen, L.; Lipson, M. On-chip gas detection in silicon optical microcavities. *Optics Express* **2008**, *16*, 4296–4301. DOI:10.1364/oe.16.004296
52. Li, J.; Qu, H.; Skorobogatiy, M. Simultaneous monitoring the real and imaginary parts of the analyte refractive index using liquid-core photonic bandgap Bragg fibers. *Optics Express* **2015**, *23*, 22963–22976. DOI: 10.1364/OE.23.022963
53. Wade, J.H.; Alsop, A.T.; Vertin, N.R.; Yang, H.; Hohnson, M.D.; Bailey, R.C. Rapid, Multiplexed Phosphoprotein Profiling Using Silicon Photonic Sensor Arrays. *ACS Central Science* **2015**, *1*, 374–382. DOI: 10.1021/acscentsci.5b00250
54. Jin, L.; Li, M.; He, J.J. Optical waveguide double-ring sensor using intensity interrogation with a low-cost broadband source. *Optics Letters* **2017**, *36*, 1128–1130. DOI: 10.1364/OL.36.001128
55. Kim, H.T.; Yu, M. Cascaded ring resonator-based temperature sensor with simultaneously enhanced sensitivity and range. *Optics Express* **2016**, *24*, 9501–9510. DOI: 10.1364/OE.24.009501
56. Jiang, X.; Chen, Y.; Yu, F.; Tang, L.; Li, M.; He, J.J. High-sensitivity optical biosensor based on cascaded Mach-Zehnder interferometer and ring resonator using Vernier effect. *Optics Letters* **2014**, *39*, 6363–6366. DOI: 10.1364/OL.39.006363
57. Wang, J.; Dai, D. Highly sensitive Si nanowire-based optical sensor using a Mach-Zehnder interferometer coupled microring. *Optics Letters* **2010**, *35*, 4229–4231. DOI: 10.1364/OL.35.004229
58. Pergande, D.; Geppert, T.M.; Rhein, A.V.; Schweizer, S.L.; Wehrspohn, R.B.; Moretton, S.; Lambrecht, A. Miniature infrared gas sensors using photonic crystals. *Journal of Applied Physics* **2011**, *109*, 083117. DOI: 10.1063/1.3575176
59. Ruth, J.H. Odor thresholds and irritation levels of several chemical substances: A review. *American Industrial Hygiene Association Journal* **1986**, *47*, A142–A151. DOI: 10.1080/15298668691389595
60. Agency for Toxic Substances & Disease Registry (ATSDR). Toxicological profile for ammonia, 2004. Available online: <http://www.atsdr.cdc.gov/> (as accessed on March 2019).
61. Chang, Y. C.; Bai, H.; Li, S.N.; Kuo, C.N. Bromocresol Green/Mesoporous Silica Adsorbent for Ammonia Gas Sensing via an Optical Sensing Instrument. *Sensors (Basel)* **2011**, *11*, 4060–4072. DOI: 10.3390/s110404060
62. Nagasaka, M.; Yuzawa, H.; Horigome, T.; Kosugi, N. Reliable absorbance measurement of liquid samples in soft X-ray absorption spectroscopy in transmission mode. *Journal of Electron Spectroscopy and Related Phenomena* **2018**, *224*, 93–99. DOI: 10.1016/j.elspec.2017.05.004
63. Content, S.; Trogler, W.C.; Sailor, M.J. Detection of Nitrobenzene, DNT, and TNT Vapors by Quenching of Porous Silicon Photoluminescence. *Chemical European Journal* **2000**, *6*, 2205–2213. DOI: 10.1002/1521-3765(20000616)6:12<2205::AID-CHEM2205>3.0.CO;2-A
64. Kazarian, S.G.; Chan, K.L.A. Chemical photography of drug release. *Macromolecules* **2003**, *36*, 9866–9872. DOI: 10.1021/ma035210l

65. Kim, S.; Pete, K.; Jeffries, J.B.; Terry, F.L.; Hanson, R.K. In situ measurements of HCl during plasma etching of poly-silicon using a diode laser absorption sensor. *Measurement Science and Technology* **2003**, *14*, 1662–1670. DOI: 10.1088/0957-0233/14/9/318
66. Tuzson, B.; Zeeman, M.J.; Zahniser, M.S.; Emmenegger, L. Quantum cascade laser based spectrometer for in situ stable carbon dioxide isotope measurements. *Infrared Physics & Technology* **2008**, *51*, 198–206. DOI: 10.1016/j.infrared.2007.05.006
67. Süess, M. J.; Hundt, P.M.; Tuzson, B.; Reidi, S.; Wolf, J.M.; Peretti, R.; Beck, M.; Looser, H.; Emmenegger, L.; Faist, J. Dual-section DFB-QCLs for multi-species trace gas analysis. *Photonics* **2016**, *3*, 24. DOI: 10.3390/photonics3020024
68. Jágerská, J.; Jouy, P.; Tuzson, B.; Looser, H.; Mangold, M.; Soltic, P.; Hugi, A.; Brönnimann, R.; Faist, J.; Emmenegger, L. Simultaneous measurement of NO and NO₂ by dual-wavelength quantum cascade laser spectroscopy. *Optics Express* **2015**, *23*, 1512–1522. DOI: 10.1364/OE.23.001512
69. Mohn, J.; Tuzson, B.; Manninen, A.; Yoshida, N.; Toyoda, S.; Brand, W.A.; Emmenegger, L. Site selective real-time measurements of atmospheric N₂O isotopomers by laser spectroscopy. *Atmospheric Measurement Techniques* **2012**, *5*, 1601–1609. DOI: 10.5194/amt-5-1601-2012
70. Fenzl, C.; Wilhelm, S.; Hirsch, T.; Wolfbeis, O.S. Optical Sensing of the Ionic Strength Using Photonic Crystals in a Hydrogel Matrix. *ACS Applied Material Interfaces* **2013**, *5*, 173–178. DOI: 10.1021/am302355g
71. Snow, P.A.; Squire, E.K.; Russell, P.S.J.; Canham, L.T. Vapor sensing using the optical properties of porous silicon Bragg mirrors. *Journal of Applied Physics* **1999**, *86*, 1781–1784. DOI: 10.1063/1.370968
72. Salem, M.S.; Sailor, M.J.; Fukami, K.; Sakka, T.; Ogata, Y.H. Sensitivity of porous silicon rugate filters for chemical vapor detection. *Journal of Applied Physics* **2008**, *103*, 083516. DOI: 10.1063/1.2906337
73. Salem, M.S.; Sailor, M.J.; Harraz, F.A.; Sakka, T.; Ogata, Y.H. Electrochemical stabilization of porous silicon multilayers for sensing various chemical compounds. *Journal of Applied Physics* **2006**, *100*, 083520. DOI: 10.1063/1.2360389
74. Michelotti, F.; Sciacca, B.; Dominici, L.; Quaglio, M.; Descrovi, E.; Giorgis, F.; Geobaldo, F. Fast optical vapour sensing by Bloch surface waves on porous silicon membranes. *Phys. Chem. Chem. Phys.* **2010**, *12*, 502–506. DOI:10.1039/b914280k